

Accession No. _____

Contract Program or Project Title: Container Assessment

Subject of this Document: CONTAINER ASSESSMENT - CORROSION STUDY OF HLW CONTAINER MATERIALS. QUARTERLY PROGRESS REPORT, April-June 1982.

Type of Document: Interim Report

Author(s): T. M. Ahn and others.

Date of Document: July, 1982

Responsible NRC Individual
and NRC Office or Division:Mr. Michael McNeil
Waste Management Branch
Division of Health, Siting and Waste Management
Office of Nuclear Regulatory Research
U. S. Nuclear Regulatory Commission
Washington, DC 20555

This document was prepared primarily for preliminary or internal use. It has not received full review and approval. Since there may be substantive changes, this document should not be considered final.

Brookhaven National Laboratory
Upton, New York 11973
Associated Universities, Inc.
for the
U.S. Department of Energy

Prepared for
U.S. Nuclear Regulatory Commission
Washington, D.C. 20555
Under Interagency Agreement DE-AC02-76CH00016
FIN A-3237

8208250029 820731
PDR RES
8208250029 PDR

NRC Research and/or Technical Assistance Rept

BNL-NUREG -31611

INFORMAL REPORT

LIMITED DISTRIBUTION

CONTAINER ASSESSMENT - CORROSION STUDY
OF HLW CONTAINER MATERIALS

QUARTERLY PROGRESS REPORT
APRIL-JUNE 1982

T. M. AHN AND P. SOO

NUCLEAR WASTE MANAGEMENT DIVISION

DEPARTMENT OF NUCLEAR ENERGY BROOKHAVEN NATIONAL LABORATORY
UPTON, NEW YORK 11973



Prepared for the U.S. Nuclear Regulatory Commission
Office of Nuclear Regulatory Research
Contract No. DE-AC02-76CH00016

NOTICE

This report was prepared as an account of work sponsored by an agency of the United States Government. Neither the United States Government nor any agency thereof, or any of their employees, makes any warranty, expressed or implied, or assumes any legal liability or responsibility for any third party's use, or the results of such use, of any information, apparatus, product or process disclosed in this report, or represents that its use by such third party would not infringe privately owned rights.

The views expressed in this report are not necessarily those of the U.S. Nuclear Regulatory Commission.

Available from
GPO Sales Program
Division of Technical Information and Document Control
U.S. Nuclear Regulatory Commission
Washington, D.C. 20555
and
National Technical Information Service
Springfield, Virginia 22161

BNL-NUREG-31611
INFORMAL REPORT
Limited Distribution

CONTAINER ASSESSMENT - CORROSION STUDY
OF HLW CONTAINER MATERIALS

QUARTERLY PROGRESS REPORT
April-June 1982

T. M. Ahn and P. Soo
Principal Investigators

Contributors:
B. S. Lee
J. Woodward
R. Sabatini

Prepared by
The Nuclear Waste Management Division
D. G. Schweitzer, Head
Department of Nuclear Energy
Brookhaven National Laboratory
Associated Universities, Inc.
Upton, NY 11973

NOTICE: This document contains preliminary information and was prepared primarily for interim use. Since it may be subject to revision or correction and does not represent a final report, it should not be cited as reference without the expressed consent of the author(s).

Prepared for the U.S. Nuclear Regulatory Commission
Office of Nuclear Regulatory Research
Contract No. DE-AC02-76CH00016
FIN No. A-3237

ABSTRACT

Three abstracts were submitted to scientific meeting on the crevice corrosion of titanium, the crevice corrosion of TiCode-12, and on the corrosion performance of TiCode-12. All of these subjects were studied for simulated WIPP brines.

Long term uniform corrosion rates were tabulated for CP titanium and TiCode-12 in WIPP brine. The potential problem of precipitation on the samples is addressed.

The mechanism of crevice corrosion for CP titanium is outlined for Brine A at 150°C. In the mechanism, macroscopic-concentration-cell formation, and the subsequent breakdown of a passive film, are considered to be responsible for crevice corrosion. To understand these phenomena, calculations of oxygen depletion rates were initiated. Also, the effect of minor constituents (Br^- , I^-) on passive-film breakdown was studied.

Samples of hydrogenated TiCode-12 were tension tested using a single-edged-notch geometry with various hydrogen concentrations. The elongation decreased gradually as the hydrogen backfill pressure was decreased. Hydrogen uptake was also measured in single coupons as well as in crevice samples. The latter showed higher hydrogen uptake.

Reproducible results for gamma radiolysis were obtained for WIPP Brine A. The calculated $G(\text{H}_2)$ values were somewhat lower than previous results obtained by Jenks in a simpler brine formulation. The probable reasons for this are discussed.

CONTENTS

ABSTRACT	iii
FIGURES.	vi
TABLES	vii
ACKNOWLEDGMENTS.	ix
1. ABSTRACT SUBMITTED TO SCIENTIFIC MEETING	1
2. UNIFORM CORROSION.	1
3. CREVICE CORROSION.	3
4. ELECTROCHEMISTRY	4
5. HYDROGEN EMBRITTLEMENT	4
5.1 Fracture Testing.	4
5.2 Hydrogen Uptake Tests	8
6. RADIATION EFFECTS.	8
7. REFERENCES	15
APPENDIX A	
APPENDIX B	
APPENDIX C	

FIGURES

1. The Amorphous X-Ray Diffraction Pattern of the Precipitates Formed During Heating of Brine A.	1
2. The Long Term Uniform Corrosion Rates of CP Titanium and Ticode-12 in Brine A.	2
3. Simulated Geometry of the Crevice Corrosion Sample Used in the Calculation	4
4. Typical Example of the Oxygen Concentration Profile With a Saturated Level of Oxygen Concentration	5
5. The Load-Displacement Curves of the Hydrogenated Single-Edged-Notched Tensile Samples	7
6. Fractographs of the Single-Edged-Notched Samples.	9
7. The Pressure Build-up During Gamma Irradiation of Brine A at a Dose Rate of Approximately 2.43×10^6 Rad/Hr	12

TABLES

1. Tensile Testing Results for Hydrogenated TiCode-12	6
2. Hydrogen Uptake Results for TiCode-12 in Brine B at 150°C	11
3. Hydrogen Uptake Results for CP Titanium in Brine B at 150°C	11
4. Analysis of Gas Generated During Gamma Radiolysis.	13
5. Calculated G Values for Overall Gas and Hydrogen	13

ACKNOWLEDGMENTS

Our thanks go to G. Spira and R. Jones for their general technical assistance, K. J. Swyler for his contributions in the radiation effects study, and P. Klotz for his work on chemical analyses. We wish to express our appreciation to E. Pinkston, C. Van Noy, and S. M. Moore for their preparation of this report, and to G. Searles for her assistance in proofreading and editing this report.

1. ABSTRACTS SUBMITTED TO SCIENTIFIC MEETING

The crevice corrosion mechanisms in CP titanium and TiCode-12 have been evaluated. Abstracts were submitted for publication to the Electrochemical Society Symposium on Crevice Corrosion and the Third Conference on Industrial Applications of Titanium, respectively. Copies of the abstracts are given in Appendices A and B. An abstract was also submitted to the MRS meeting on the corrosion performance of TiCode-12 in a WIPP brine (Appendix C).

2. UNIFORM CORROSION

Continuing efforts were made to obtain long term data on uniform corrosion rates for times up to 200 days. As reported previously,¹ the formation of precipitates on the samples upon solution heating makes it difficult to obtain reproducible corrosion-rate data. These precipitates were identified as an amorphous compound of Mg and Si by EDAX probe and X-ray diffraction. The amorphous X-ray diffraction pattern is shown in Figure 1.

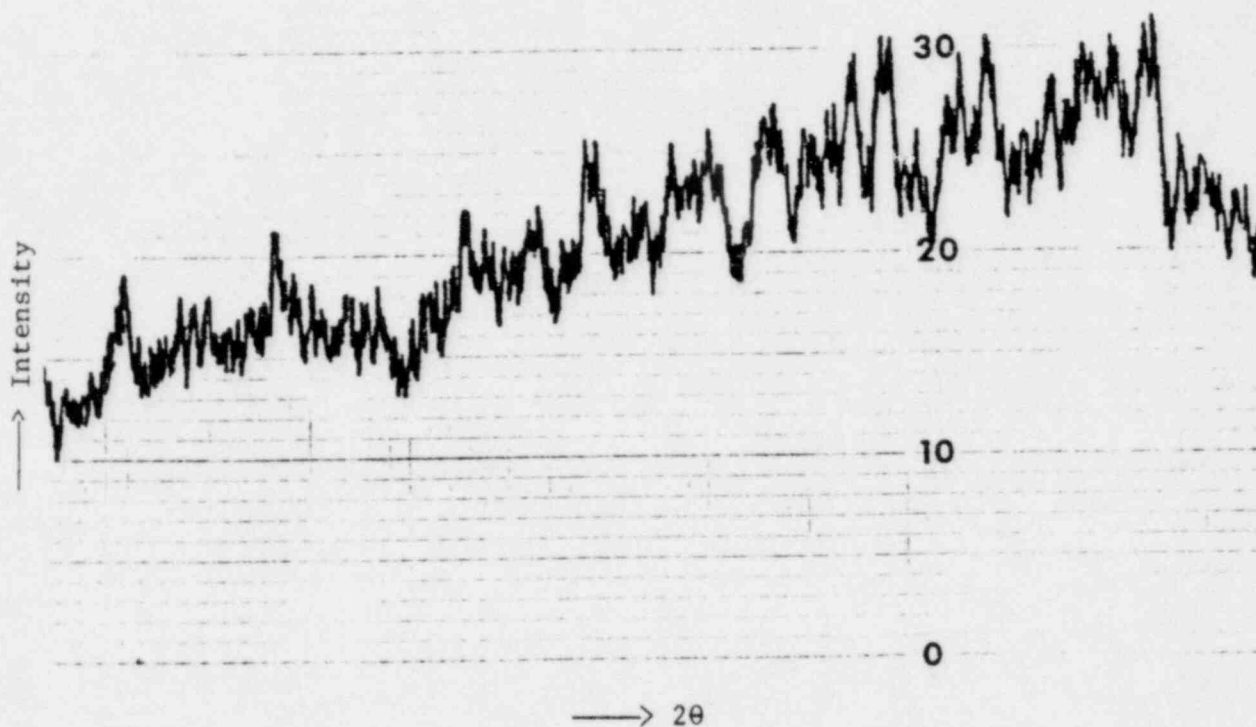


Figure 1. The amorphous X-ray diffraction pattern of the precipitates formed during heating of Brine A.

Figure 2 shows two sets of weight gain data, one with the deposits and the other with deposits removed by scraping with filter paper. The complications arising from compound formation make it difficult to interpret the data on a mechanical basis.

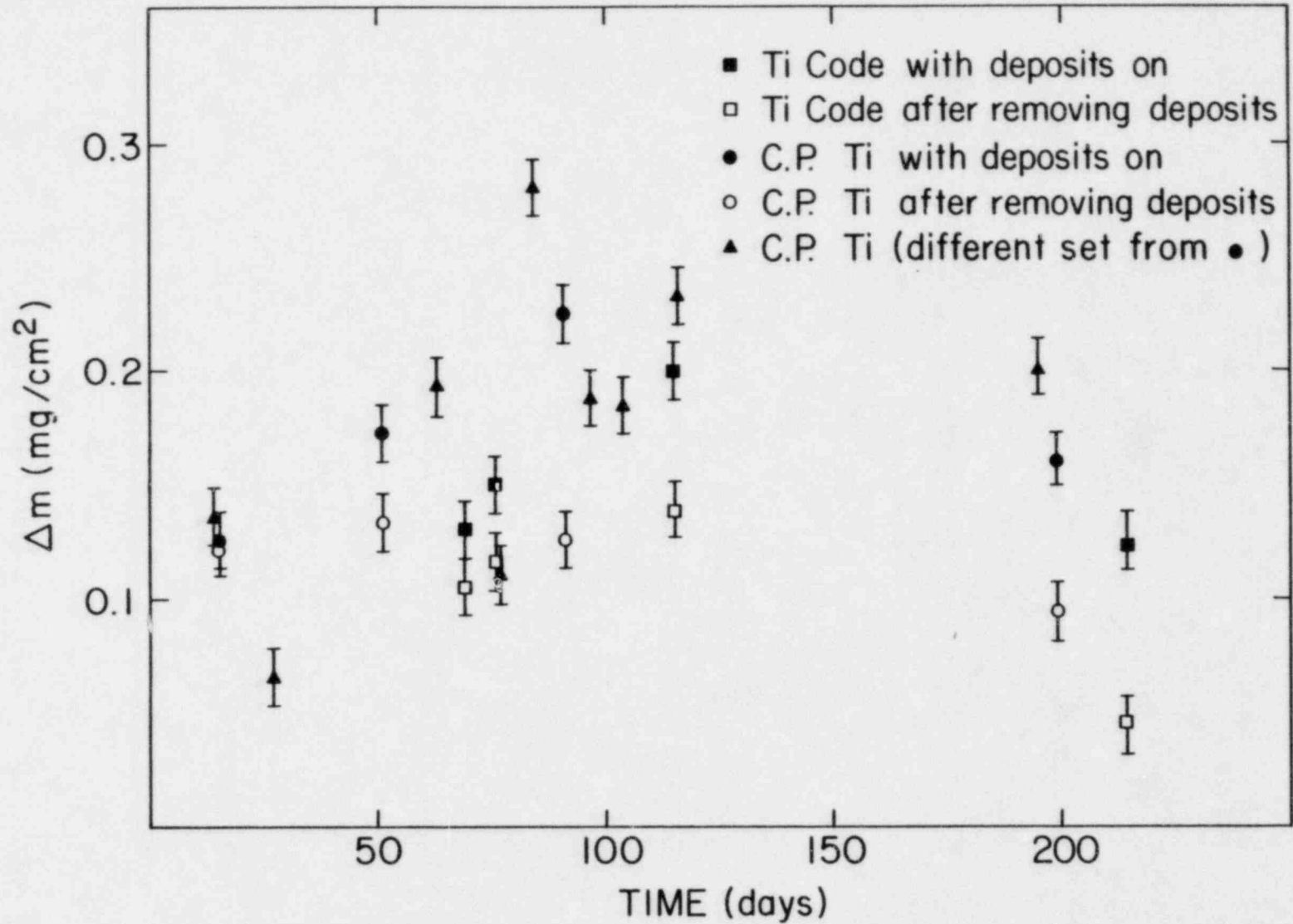


Figure 2. The long term uniform corrosion rates of CP titanium and TiCode-12 in Brine A.

The planned long term testing will be continued using a different sample design (bigger samples hung vertically) to avoid the precipitation problem.

3. CREVICE CORROSION

The crevice corrosion mechanism for CP titanium has been investigated for WIPP Brine A at 150°C. The work was performed to gain a basic understanding of the crevice corrosion mechanism for TiCode-12. Metal-metal crevices showed the anatase form of TiO₂ scale with traces of Ti₃O₅, while metal teflon crevices showed severe corrosion resulting in the rutile form of TiO₂ scale. Macroscopic concentration cell formation, and the subsequent breakdown of the passive film, are considered to be the mechanism of the crevice corrosion of CP titanium in Brine A at 150°C. The details of this process are given in Appendix A.

The first stage of crevice corrosion is oxygen depletion inside the crevice. A calculation of oxygen depletion rates was initiated to understand the process in this region. Figure 3 shows the idealized geometry of the crevice sample used in the calculation. Oxygen is consumed in the crevice by the cathodic reaction of uniform corrosion. A shallow crevice leads to a gradual decrease of the oxygen level inside the crevice because of the limited velocity of the oxygen diffusion into the crevice from the bulk solution. Using a mass balance of the oxygen inflow and cathodic consumption in an infinitesimal area, we may write the oxygen concentration *c* at time *t* in a radial position *r* as:

$$\frac{\partial c}{\partial t} = D \frac{\partial^2 c}{\partial r^2} + \frac{D}{r} \frac{\partial c}{\partial r} - \frac{CR \cdot \rho \cdot [AW(O_2)/AW(TiO_2)]}{8 \cdot dg} \quad (1)$$

We assume that the concentration is symmetrical with a negligible amount of angular flux, and that the oxide formed inside the crevice is TiO₂. *D* is the oxygen diffusivity in the solution, *CR* is the corrosion rate, ρ is the density of the oxide, *dg* is the crevice gap and *AW*(O₂) and *AW*(TiO₂) are atomic weights of O₂ and TiO₂, respectively. The initial and boundary conditions are:

$$\begin{aligned} c &= c_0 \text{ at } t = 0 \\ \frac{\partial c}{\partial r} &= 0 \text{ at } r = 0 \\ c &= c_0 \text{ at } r = r_0 \end{aligned} \quad (2)$$

where *c*₀ is the initial concentration of oxygen dissolved in the bulk solution. These equations were evaluated using the mathematical code PDECOL² developed with a finite element collocation method.

Initially, the calculation was performed for a 1-cm radius sample with various (*CR*/*dg*) ratios. The oxygen diffusivity 2.62 x 10⁻⁴ cm²/sec, (Reference 3) at 150°C, ρ 3.84 g/cm³ for the anatase form of TiO₂,⁴ a

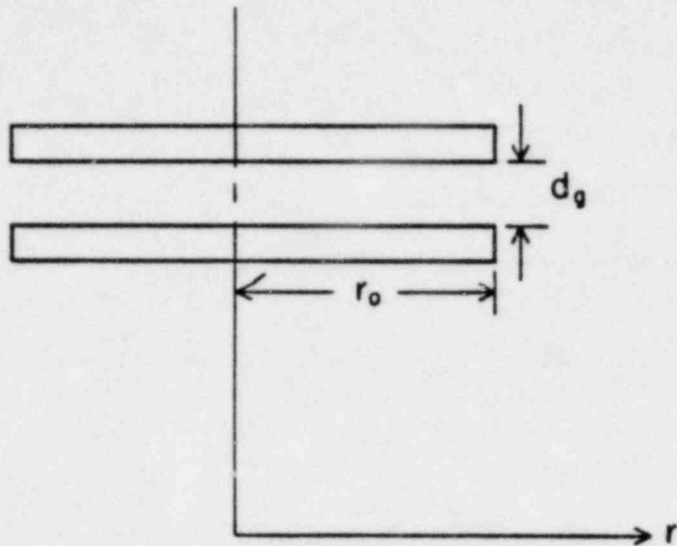


Figure 3. Simulated geometry of the crevice corrosion sample used in the calculation.

constant corrosion rate $1 \mu\text{m}/\text{year}$. For $d_g = 10 \mu\text{m}$ which is the approximate mean gap of the crevice in our experiment, the oxygen depletion is negligible.

However, the corrosion rate is very high initially and the bolted region of the crevice may have a very shallow crevice gap less than $10 \mu\text{m}$. Both of these effects may enhance the oxygen depletion rate. An example is shown in Figure 4 where $\text{CR}/d_g = 1.26 \times 10^{-2}/\text{day}$ was used. The significant oxygen depletion as well as oxygen saturation at a concentration level below c_0 are observed. When the CR/d_g ratio is increased further, complete depletion in the center was obtained. At the present time, neither the minimum d_g values nor CR kinetics are available. Currently we are generating these values experimentally and the subsequent reevaluation of Equation (1) is under way.

4. ELECTROCHEMISTRY

The study of I^- and Br^- effects on the open circuit corrosion potential was initiated at a test temperature of 80°C . Standard Brine A was prepared for all tests except those with Br^- and I^- contents. The I^- and Br^- ions were added during the measurement of the corrosion potential. Up to this time, no appreciable potential change was observed. The probable reason for this is the presence of I^- and Br^- ions as impurities which make the effects of intentionally added I^- and Br^- undetectable. This work will be continued.

5. HYDROGEN EMBRITTLEMENT

5.1 Fracture Testing

The testing of single-edged-notched tensile specimens was continued for various hydrogen concentration levels. By fatigue precracking the specimens

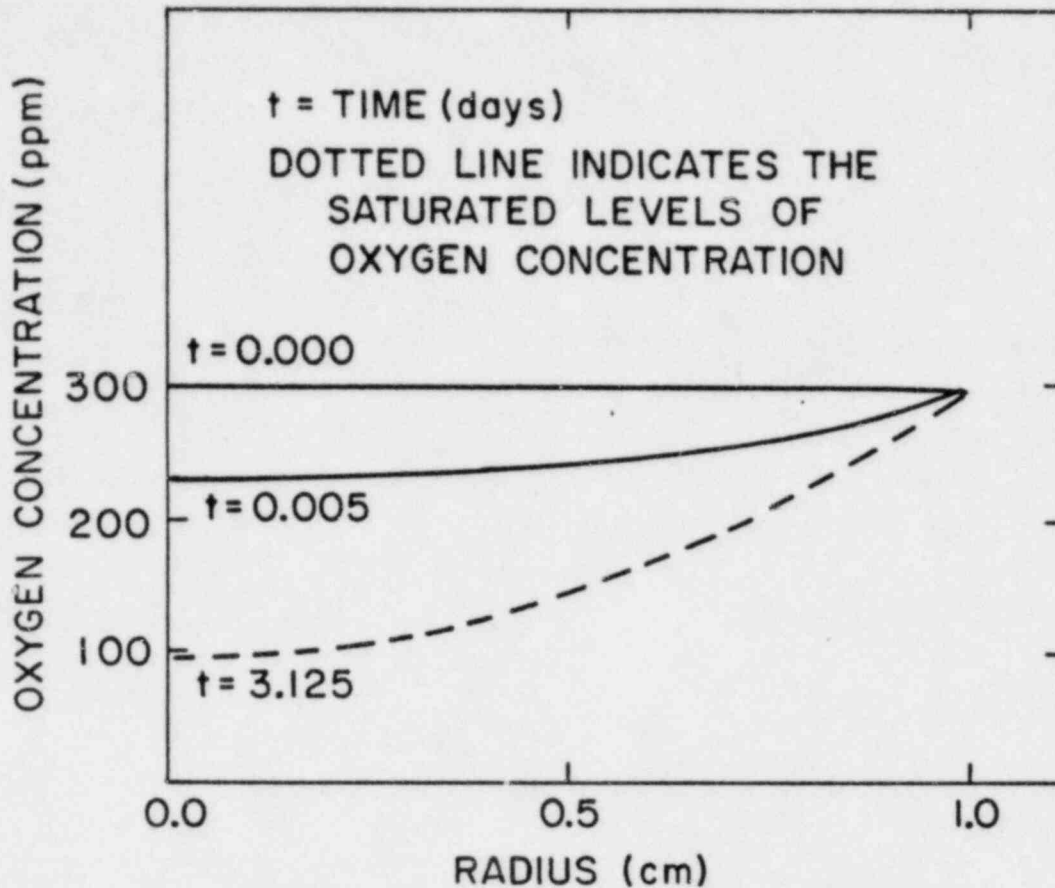


Figure 4. Typical example of the oxygen concentration profile with a saturated level of oxygen concentration.

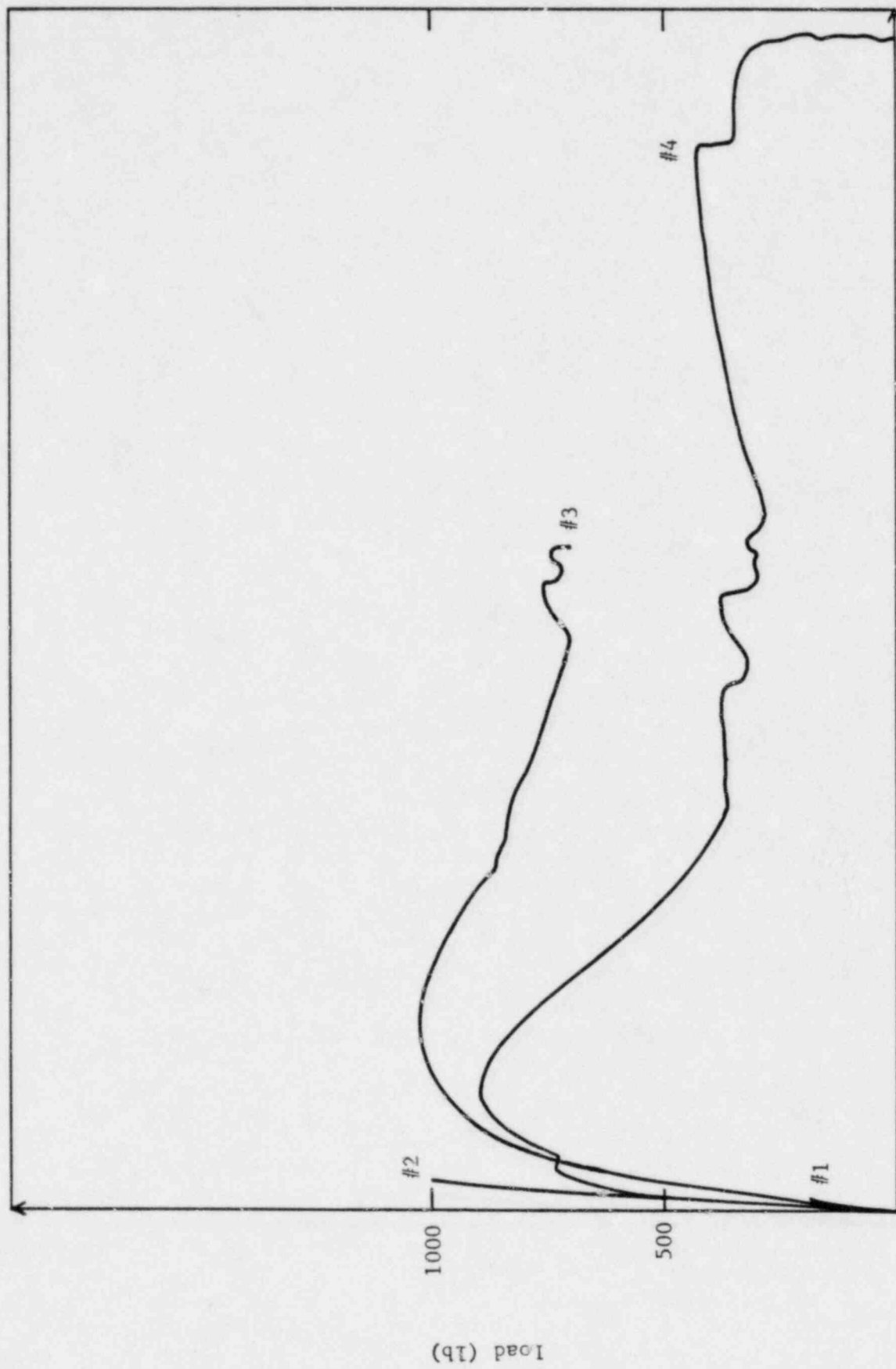
at cyclic loads between 50 lbs tension and 500 lbs tension at 20 Hz, the previously reported crack blunting problem was eliminated. Also, a new specimen geometry (3.00" x 0.75" x 0.10") was used with a ratio of crack length to specimen width of 0.5. The hydrogenation of the samples was performed by heating the samples in a vacuum furnace backfilled with ultra-high-purity hydrogen. The heating condition was 750°C for five hours at hydrogen pressures of 1/4 atm, 20 mm Hg, 500 $\mu\text{m Hg}$ and 30 $\mu\text{m Hg}$. The specimens were tension tested to failure at a crosshead speed of 0.005 cm/min. The load-displacement curves were obtained and the plane-strain-threshold stress intensity was calculated, if it existed, using the formula by Tada,⁵ which eliminates the uncertainty in the Poisson ratio. The hydrogen concentration for each sample is being analyzed.

Table 1 shows the experimental conditions and the results, and Figure 5 shows the load-displacement curves of the samples. The elongation is increased as the hydrogen backfill pressure is decreased (Samples 2-4). For large hydrogen backfill pressures (Samples 1 and 2), negligible ductility is observed and the plane strain condition is used to obtain the approximate threshold stress intensity. The fractographs of Samples 1 and 2 show alpha-beta

Table 1

Tensile Testing Results for Hydrogenated TiCode-12

Sample	Hydrogen Backfill Pressure (mm Hg)	Maximum Load (lb)	Macroscopic Morphology	Fractograph	Notes
1	190	180	Flat	Fig. 6a	$K_Q=K_{th}=9.5\text{MPa}\sqrt{\text{m}}$
2	20	1000	Flat	Fig. 6b	$K_Q=K_{th}=52.5\text{MPa}\sqrt{\text{m}}$
3	0.5	1020	Flat and minor shear lip.	Fig. 6c	Non-plane-strain condition.
4	0.03	900	Flat and minor shear lip.	Fig. 6c	Non-plane strain condition.



Displacement (Arbitrary Units)

Figure 5. The load-displacement curves of the hydrogenated single-edged-notched tensile samples.

interfacial separation and crystallographic fracture (Figures 6a and 6b), while samples 3 and 4 show quasi-cleavage of alpha-grains (Figures 6c and 6d). Thin foil preparation, as well as hydrogen analysis, are being performed to further evaluate this behavior.

5.2 Hydrogen Uptake Tests

In the previous quarterly report,¹ we reported that hydrogen uptake tests were under way. The samples were single coupons, as well as creviced samples, and they are being used to check the enhanced hydrogen uptake rate caused by the breakdown of the passive film inside the crevice. Samples were tested at 150°C in WIPP Brine B in the presence of hydrogen at a room temperature pressure of 220 psi.

As shown in Tables 2 and 3 the single coupons uptake an appreciable amount of hydrogen, especially in CP titanium. The poor reproducibility implies that the initial state of the air-formed oxide may have played an important role. Furthermore, the reducing environment caused by the hydrogen seems to have slowed down oxide scale growth in the aqueous environments which leads to the enhanced hydrogen uptake. The most important finding is that the enhanced hydrogen uptake rate in the crevice sample is probably caused by the breakdown of the passive film inside the crevice.

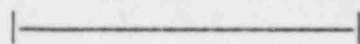
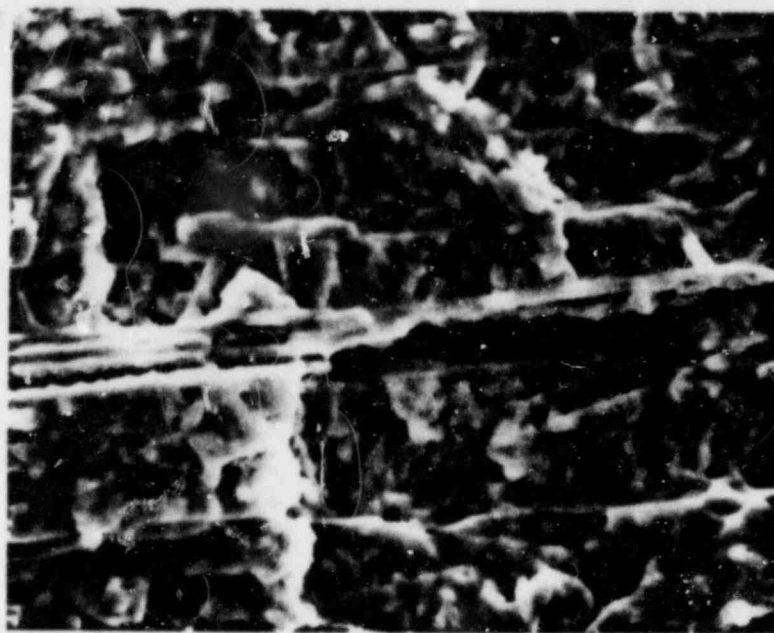
6. RADIATION EFFECTS

Reproducible results on gamma radiolysis were obtained for WIPP Brine A. In the analysis of gases generated, the previously reported problem of inhomogeneous gas distribution was overcome by evacuating the gas generated with a mechanical pump. Not only light gases, but also heavy ones, were extracted from the irradiation cell for analysis. Figure 7 shows the pressure build-up during irradiation at a dose rate of approximately 2.43×10^6 rad/hr. Table 4 shows the results of the analysis of gas generated, and preliminary calculations of G values are shown in Table 5. The following equation was used in the calculation:⁶

$$G = \frac{V_p}{M_s} \frac{\Delta P}{\Delta \phi} \frac{T_0}{T} 2.93 \times 10^6 \quad (3)$$

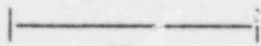
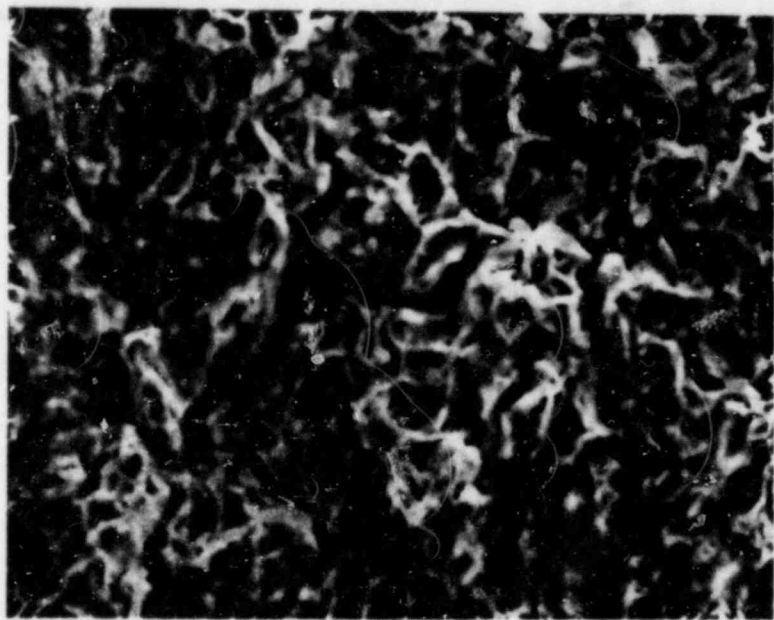
where V_p is the plenum volume of the test cell, (cm^3) M_s is the sample weight (gm), $(\Delta P/\Delta \phi)$ is the slope of the curve of pressure vs. radiation dose (psi/rad), T_0 is 273.16°K, and T is the irradiation temperature (°K). T was taken to be 293°K.

The ratios of the major gases generated are reproducible as seen in Table 4. At one-half of the total dose (Sample 2), the gases generated are not one half of the gases in Sample 1, which implies that gases are not generated linearly with the total dose. This work is currently being repeated for confirmation. The calculated $G(\text{H}_2)$ values are quite low compared to the $G(\text{H}_2)$ values reported previously by Jenks for NaCl-saturated brines with additions of MgCl_2 and NaBr .⁷ In the irradiation of Jenks' brines,



5 μ

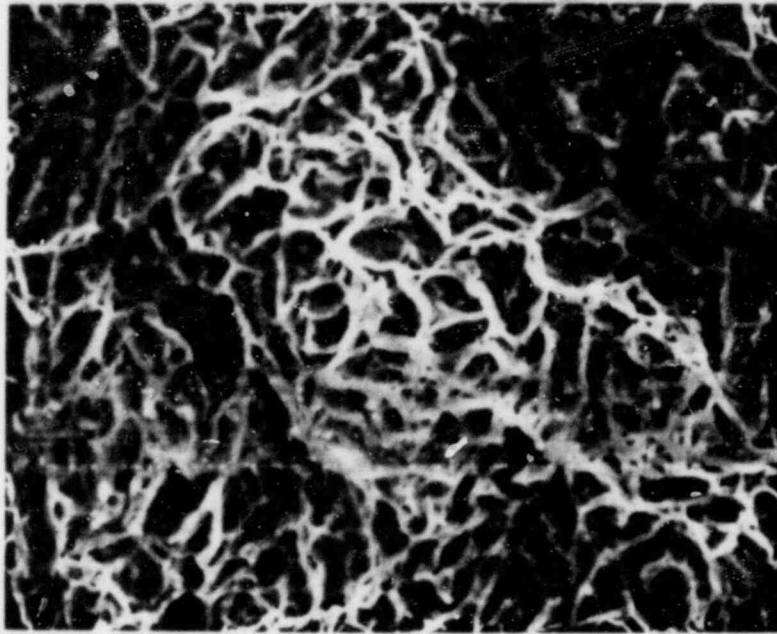
(a)



50 μ

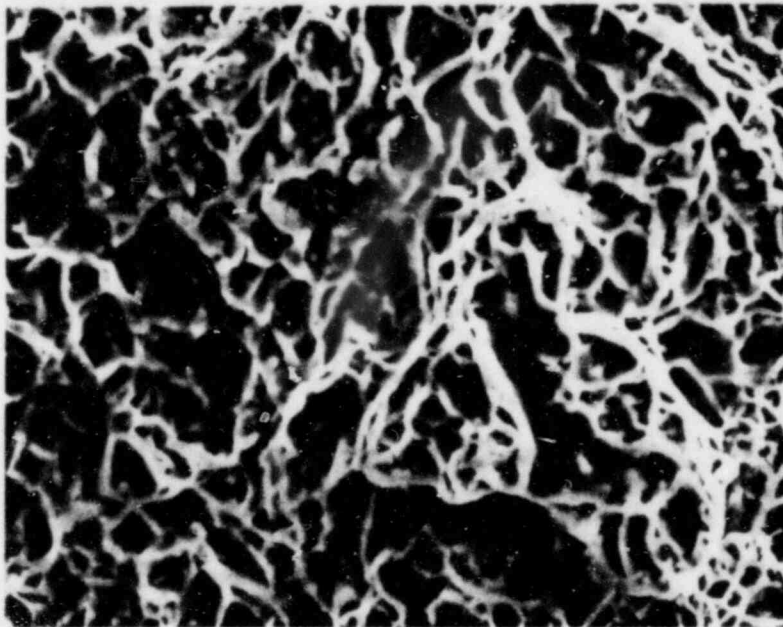
(b)

Figure 6. Fractographs of the single-edged-notched samples.



|—————|
50 μ

(c)



|—————|
2 μ

(d)

Figure 6. Fractographs of the single-edged-notched samples.

Table 2

Hydrogen Uptake Results For TiCode-12 in Brine B at 150°C

Run	Single Coupon	Crevice Sample	
1	65.8	80.6	91.2
2	32.5	74.4	

Note: The hydrogen concentration is 34 ppm in the as-received alloy.

Table 3

Hydrogen Uptake Results For CP Titanium in Brine B at 150°C

Run	Single Coupon	Crevice Sample	
1	174.2	186.2	
2	139.0	395.0	

Note: The hydrogen concentration is 74 ppm in the as-received metal.

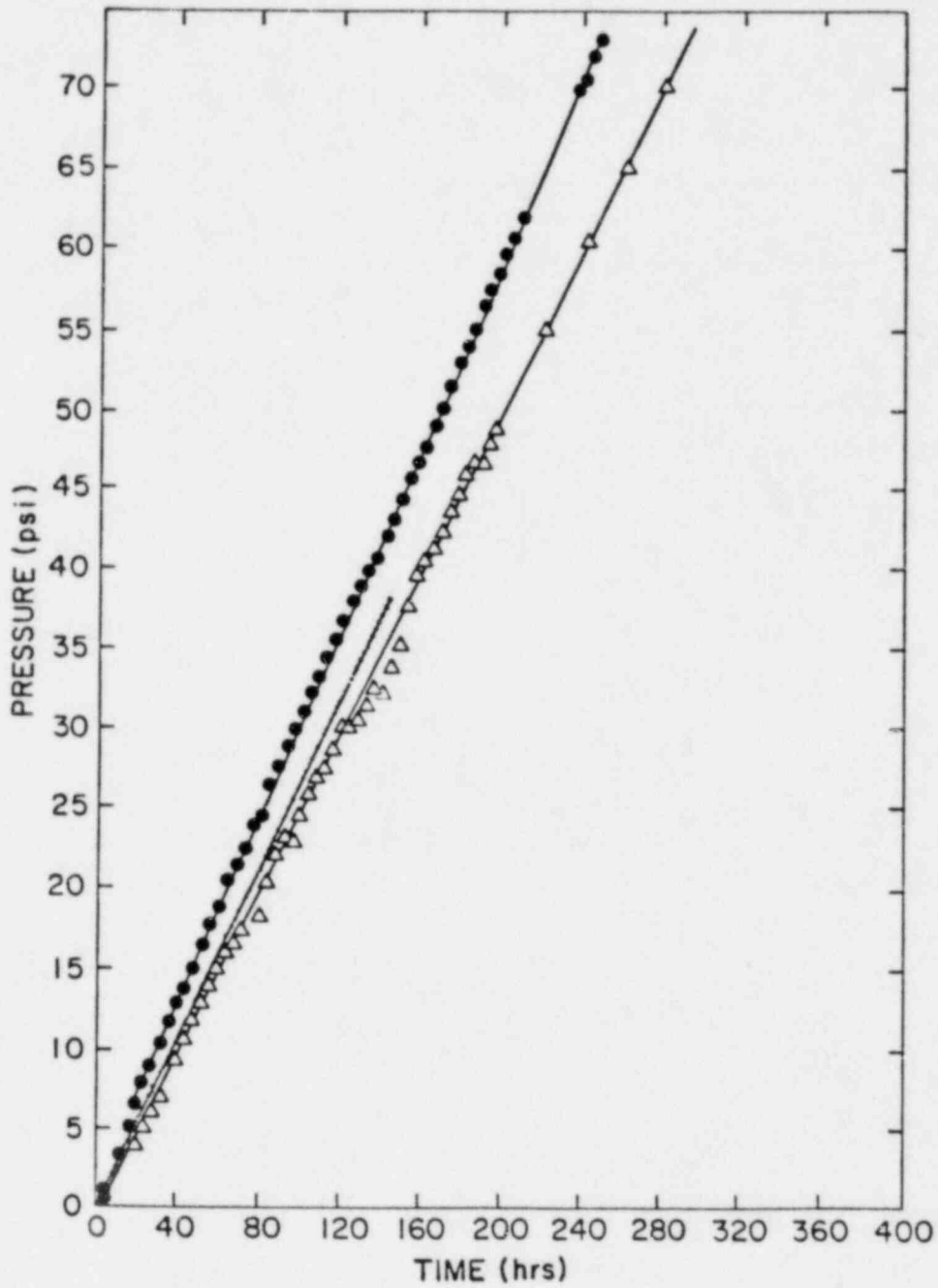


Figure 7. The pressure build-up during gamma irradiation of Brine A at a dose rate of approximately 2.43×10^6 rad/hr.

Table 4

Analysis of Gas Generated During Gamma Radiolysis

Sample No.	Total Dose (rad x 10 ⁻⁸)	Pressure Percentage							
		H ₂	O ₂	N ₂	CO ₂	H ₂ O	Ar	He	CH ₃ OH
1-run 1	6.95	58.23	21.62	3.62	2.85	0.23	0.05	11.60	1.74
1-run 2	7.39	58.97	26.72	4.54	0.49	0.32	0.06	8.90	--
		60.35	25.01	5.05	0.45	0.40	0.05	8.68	--
2-run 1	3.55	41.70	10.08	20.62	6.66	0.41	0.26	9.41	10.86

Table 5

Calculated G Values for Overall Gas and Hydrogen

Sample	G (Overall)	G(H ₂)
1-run 1	0.33	0.19
1-run 1	0.37	0.22, 0.22
2-run 1	0.35	0.14

G(H₂) ranged from 0.4 to 0.7. The majority of his experiments were performed in a helium environment and irradiation temperatures ranged from 30 to 182°C. Also, the solute species and concentrations are quite different from those used in the current program. The present experiment was performed at 20°C in air. In Jenks' experiments, certain solutions showed G(H₂) values as low as ours for irradiation at 30 to 45°C. Therefore, our results are not unusual. At the present time, we consider that the following three factors (taken from Reference 9) may be the reasons for our low values for G(H₂):

1. Recombination of gases as condensates on the low-temperature cell wall may have reduced the molecular yield.
2. The presence of oxygen may have lowered the hydrogen yield by a "scavenging effect".

3. The increased concentration of active solutes may have reduced the molecular yield.

Currently, experiments in He environments and experiments at higher temperatures are planned to study further the solute and environmental effects.

7. REFERENCES

1. T. M. Ahn and P. Soo, "Container Assessment - Corrosion Study of HLW Container Materials, Quarterly Progress Report," Brookhaven National Laboratory Report, BNL-NUREG-51449, Vol. 1 No. 1, 2 and 3, 1981, Vol. 1 No. 4, Vol. 2 No. 1, 1982.
2. N. K. Madsen and R. F. Sincovec, "PDECOL: General Collocation Software for Partial Differential Equations," Lawrence Livermore Laboratory, UCRL-78263, 1976.
3. D. M. Himmelblau, "Diffusion of Dissolved Gases in Liquids," Chem. Rev. 64, 527 (1964).
4. Handbook of Chemistry and Physics, Sixty-Second Edition, CRC Press, 1981.
5. H. Tada, The Stress Analysis of Cracks Handbook, Del Research Corporation, 1973.
6. R. E. Barletta, K. J. Swyler, S. F. Chan and R. E. Davis, "Solidification of Irradiated EPICOR-II Waste Products," Draft Report, BNL-NUREG-29913, 1981.
7. G. H. Jenks and J. R. Walton, "Radiation Chemistry of Salt-Mine Brines and Hydrates," ORNL-5726, Oak Ridge National Laboratory, 1981.
8. G. H. Jenks, private communication.
9. A. O. Allen, The Radiation Chemistry of Water and Aqueous Solutions, D. Van Nostrand Co., 1961.

APPENDIX A

CREVICE CORROSION OF TITANIUM IN A BRINE SOLUTION*

B. S. Lee, T. M. Ahn and P. Soo
Brookhaven National Laboratory
Upton, NY 11973

Introduction

Crevice corrosion of titanium in a concentrated brine solution was studied at a test temperature of 150°C. The work was performed to gain a basic understanding of the crevice corrosion mechanism for a dilute titanium alloy, TiCode-12 (Ti-0.3 Mo-0.8 Ni) which is a candidate container material for the geological isolation of high level nuclear waste.¹

Results

In the current work titanium-titanium and teflon-titanium-teflon crevice samples were prepared. Each element measured 2x1x0.05 cm and they were held together by a titanium bolt passing through the center of the pieces. Samples were exposed for periods up to two months in Brine A, typical of that at the Waste Isolation Pilot Project site in New Mexico which contains 42,000 ppm Na⁺, 30,000 ppm K⁺, 35,000 ppm Mg⁺², 600 ppm Ca⁺², 190,000 ppm Cl⁻, 3,500 ppm SO₄²⁻ and 1,200 ppm BO₃⁻.

Metal-metal crevices showed only oxide scale thickening at the center of the crevice while metal-teflon crevices showed severe corrosion.

A transmission electron microscope (TEM) study showed that the scale which formed inside the metal-metal crevices is made up of crystals of the anatase form of TiO₂. Traces of Ti₃O₅ were also identified. The amount of this lower oxide increases at locations near the center of the crevice.

In the case of severe crevice corrosion, the corrosion product was identified as a rutile form of TiO₂ by Griess.² In one of our teflon-titanium-teflon specimens, exposed to brine for two months at 150°C, a concentric ring of corroded metal was found at the center of the crevice extending to a distance of about 2 mm from the bolt hole. This was caused by active titanium dissolution. This area was surrounded by aggregates of very fine crystals (2000-3000 Å as shown in Figure 1) which could, based on Griess' work, be the rutile form of TiO₂. From the morphology of the aggregates, it is apparent that these are precipitated from the solution. Adjacent to these aggregates, on the side closer to the perimeter of the crevice, large anatase crystals (1-3 μm, as shown in Figure 2) were identified by electron diffraction in the TEM. The anatase often occurs in the presence of very fine crystals (~2000 Å in diameter). Still further out from these crystals were compact

*This work was performed under the auspices of the United States Nuclear Regulatory Commission.

crystals of anatase. These showed signs of transformation to smaller crystals in some locations.

Discussion

Based on these observations, and electrochemical studies of other workers,^{3,4} it is postulated that anatase crystals initially grow inside the crevice, causing oxygen depletion and eventually forming a macroscopic concentration cell. As the oxygen depletion process proceeds the pH and electrode potential decrease and more Ti_3O_5 either forms or is transformed from the anatase. Some of this dissolves into the electrolyte as Ti(III) or Ti(IV) ions. The Ti(III) has been postulated to accelerate the dissolution of titanium in both active and passive regions.³

We believe that at the onset of breakdown of the anatase film at the center of the crevice, Ti(II) ions from the active dissolution of Ti begin to migrate outward. When these ions reach a site with the appropriate pH/potential condition, they precipitate as rutile.

With respect to the electrochemical aspects of crevice corrosion a potential drop has been observed after oxygen depletion by Diegle.⁴ He measured the crevice corrosion cell current and potential as functions of exposure time at 150°C in neutral brine. For the first 100 minutes he showed that the potential increased slowly, moving in the noble direction. However, the current did not change significantly, indicating that the anatase scale was growing in thickness. At the end of this stage, the potential begins to decrease and the current increases. Probably, the pH drop and oxygen depletion causes the potential drop. As a result, Ti_3O_5 begins to form and breakdown of the compact anatase film is initiated.

We are currently estimating crevice parameters which influence oxygen depletion rates and attendant pH changes in our system. Our calculations using a mathematical model show that initial oxygen depletion time is a strong function of the crevice gap size and temperature. Furthermore, our experimental conditions can cause complete oxygen depletion in the center of the crevice.

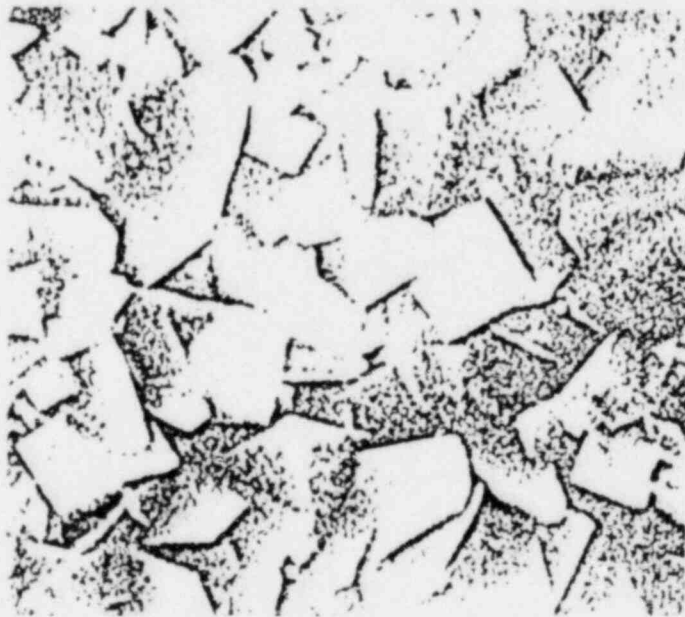
References

1. T. M. Ahn, et al, "Container Assessment - Corrosion Study of HLW Container Materials, Quarterly Progress Report, January-March 1982," Brookhaven National Laboratory, BNL-NUREG-51449, Vol. 2, No. 1, 1982.
2. J. C. Griess, "Crevice Corrosion of Titanium in Aqueous Salt Solutions," Corrosion 24, 96 (1968).
3. N. T. Thomas and Ken Nobe, "Electrochemical Behavior of Titanium," J. Electrochem. Soc. 119, 1450 (1972).
4. R. B. Diegle, "New Crevice Corrosion Test Cell," Mat. Perform. 21, 43 (1982).



|————|
10 μ

Figure 1. Scanning Electron Microscope (SEM) micrograph of aggregates of fine titanium oxide crystals deposited inside the metal-teflon crevice. This is thought to be rutile.



|————|
5 μ

Figure 2. SEM micrograph of larger crystals of anatase inside the metal-teflon crevice.

APPENDIX B

Identification of Crevice Corrosion in Titanium Alloy TiCode-12 in Neutral Brine Solution at 150°C*

T. M. Ahn, B. S. Lee, J. Woodward and P. Soo
Brookhaven National Laboratory
Upton, NY 11973

ABSTRACT

There is currently in the U.S.A. an effort to develop titanium alloy TiCode-12 (nominal composition: 0.80 weight percent Ni, 0.3 weight percent Mo and the balance Ti) as the prime corrosion resistant material for high level waste containers which will be emplaced in mined geologic repositories. Preliminary data indicate that although uniform corrosion is unlikely to present a problem with respect to failure of the container, little information is available on possible localized corrosion failure mechanisms such as crevice corrosion and hydrogen embrittlement. This paper outlines initial results on the crevice corrosion of TiCode-12 in simulated rock salt brine solutions at and above 150°C. The results will be used for the long term prediction and assessment of crevice corrosion attack of TiCode-12 waste containers which are situated in a rock salt repository. A distinct corrosion product (violet blue or yellow color) was observed in a mechanically simulated crevice after two- to four-weeks exposure. Increasing temperature accelerated the reaction rates and deaerated solutions gave less corrosion than aerated ones. There was an indication of cation depletion inside the crevice. TEM analysis of the oxide film inside the crevice showed TiO₂ was predominant, with a trace of lower oxides. These results are consistent with those expected from the unified theory of crevice corrosion, and consequently confirm the existence of crevice corrosion of TiCode-12 in near neutral brine solutions at 150°C. In order to evaluate the specific operating corrosion mechanisms, commercially pure titanium was also studied. At least two hypotheses may be considered at the present time: (1) the degree of polarization is different within the crevice, (2) the hydrolysis of dissolved metal ions takes place. The role of alloying elements, Mo and Ni, will be discussed with respect to these hypotheses.

*This work was carried out under the auspices of the U. S. Nuclear Regulatory Commission.

APPENDIX C

Corrosion of TiCode-12 in a Simulated Waste Isolation Pilot Project (WIPP) Brine*

T. M. Ahn, B. S. Lee, J. Woodward,
R. L. Sabatini and P. Soo
Brookhaven National Laboratory
Upton, NY 11973

ABSTRACT

The corrosion behavior of TiCode-12 (Ti-0.3 Mo-0.8 Ni) high level waste container alloy has been studied for a simulated WIPP brine at temperatures up to 150°C. Crevice corrosion was identified as a potentially important failure mode for this material. Within a mechanical crevice, a thick oxide film was found and shown to be the anatase form of TiO_2 , with smaller amounts of Ti_3O_5 also present. Acidic conditions were found to cause a breakdown of the passive oxide layer. Increasing temperature and solution aeration accelerate the corrosion rate. The incubation time for crevice corrosion has been calculated for various test conditions. In hydrogen embrittlement studies, it was found that hydrogen causes a significant decrease in the threshold stress intensity level in fracture mechanics samples. Hydride formation is thought to be responsible for crack initiation. Gamma irradiation studies were performed in WIPP brine and the potential for radiolysis products to induce failure in TiCode-12 has been addressed. Attention has also been given to methods for extrapolating short term uniform corrosion rate data to extended times, in order to predict container performance.

*This work was performed under the auspices of the United States Nuclear Regulatory Commission.

Review Summary

The corrosion behavior of TiCode-12 (Ti-0.3 Mo-0.8 Ni) high level waste container material has been studied in a simulated Waste Isolation Pilot Project (WIPP) brine environment,^{1,2} for temperatures up to 150°C. Various corrosion failure modes have been investigated with current principal emphasis being on crevice corrosion and hydrogen embrittlement effects. A limited amount of work has also been focused on radiolysis effects in brine, stress corrosion cracking, uniform corrosion, and pitting.

The work on crevice corrosion was initiated because of the potential for crevice type environments being formed between the TiCode-12 container and surrounding backfill materials or metallic emplacement sleeves. Experiments using metal/metal and metal/teflon crevice samples showed that thick multi-colored oxide films were formed in WIPP brine for exposures up to two months at 150°C. Electron diffraction analysis carried out in a transmission electron microscope shows that the corrosion products are primarily made up of the anatase form of TiO₂ with much smaller amounts of Ti₃O₅ also present. Increasing temperature and increased O₂ concentration increase the corrosion rate. Measurements of the open-circuit potentials at 80°C show that there is a breakdown of the passive film as the pH of the brine falls below one. The pH drop is expected to occur in the crevice. Work on pure titanium was also carried out to provide additional data on the crevice corrosion mechanism.

The deleterious effects of hydrogen on the mechanical properties of TiCode-12 have been investigated since this material typically contains 30 ppm of hydrogen as a residual element. Furthermore, radiolysis of the groundwater may also cause an increase in the hydrogen level in the alloy. Slow-strain-rate embrittlement and impact embrittlement have been observed in cathodically charged specimens in tension and bend tests.¹ Fractographic analysis of the specimens with a scanning electron microscope showed that interfacial separation between the alpha and beta phases appears below the hydrogen level at which cleavage occurs. Single-edged-notched fracture mechanics samples were used to obtain the apparent stress intensity factors at 2% crack extension for samples containing hydrogen levels in excess of 5000 ppm. The apparent stress intensity factor was found to decrease by a factor of about 10 to approximately 5 MPa $\sqrt{\text{m}}$ after hydrogenation. Fractographs show both alpha phase crystallographic fracture and alpha-beta interface cracking. These observations imply that the formation of hydride is responsible for crack initiation. Based on the hydride formation mechanism, a model is currently being developed to predict the crack initiation time for prototypic repository conditions.

Acidified brine formed by crevice corrosion can induce other corrosion failure modes such as stress corrosion cracking, pitting, and hydrogen uptake after breakdown of the passive film. These modes are unlikely to occur in neutral brines.² To study these phenomena, immersion tests on C-rings and unstressed specimens are being performed. Enhanced hydrogen uptake has been observed in crevice coupons compared to single coupons.

Measurements have been made of the pressure buildup during gamma-ray irradiation of the WIPP brine at a dose rate of $\sim 4 \times 10^6$ rad/hr and a total dose of 1.2×10^9 rads. The gas generated contains about 58% hydrogen. The irradiated solution is being analyzed for oxidants such as ClO_3^- and H_2O_2 . The effect of these oxidizers on open-circuit corrosion has been measured at room temperature. A potential rise has been observed, which is a possible indication of enhanced susceptibility to stress corrosion cracking.

Uniform corrosion has been studied as a function of time using immersion tests at 150°C . The results are in reasonable agreement with previous data.^{2,3} It was found that direct correlation between weight gain and the oxide thickness may be difficult because of salt deposition on the samples and/or possible compound formation. In the extrapolation of these results to extended times, oxide growth kinetics should be used because the corrosion rate is highest during the initial stages of attack.

Acknowledgments

The authors gratefully acknowledge the assistance of G. Spira, R. Jones, K. Swyler, R. Newman, J. Forrest, and P. Klotz in much of the experimental work.

References

1. T. M. Ahn and others, Brookhaven National Laboratory, "Container Assessment - Corrosion Study of HLW Container Materials, Quarterly Progress Report," NUREG/CR-2317, BNL-NUREG-51449, Vol. 1, Nos. 1-4, 1981 and Vol. 2, No. 1, 1982.
2. M. A. Molecke, D. W. Schaefer, R. S. Glass, and J. A. Ruppen, "Sandia HLW Canister/Overpack Studies Applicable for a Salt Repository," SAND 81-1585, 1981.
3. R. E. Westerman, "Investigation of Metallic, Ceramic, and Polymeric Materials for Engineered Barrier Applications in Nuclear-Waste Packages," PNL-3484, 1980.